Available online at www.sciencedirect.com
ScienceDirect
Journal of Solid State Chemistry 180 (2007) 2202–2208
JOURNAL OF SOLID STATE CHEMISTRY
www.elsevier.com/locate/jssc

Synthesis, structure and properties of $SrAu_3In_3$ and $EuAu_3In_3$—New indides with gold zig-zag chains

Ihor R. Muts[a,b], Falko M. Schappacher[a], Wilfried Hermes[a], Vasyl' I. Zaremba[b], Rainer Pöttgen[a,*]

[a]*Institut für Anorganische und Analytische Chemie, Universität Münster, Corrensstrasse 30, D-48149 Münster, Germany*
[b]*Inorganic Chemistry Department, Ivan Franko National University of Lviv, Kyryla and Mephodiya Street 6, 79005 Lviv, Ukraine*

Received 21 March 2007; received in revised form 3 May 2007; accepted 19 May 2007
Available online 5 June 2007

Abstract

New indides $SrAu_3In_3$ and $EuAu_3In_3$ were synthesized by induction melting of the elements in sealed tantalum tubes. Both indides were characterized by X-ray diffraction on powders and single crystals. They crystallize with a new orthorhombic structure type: *Pmmn*, $Z = 2$, $a = 455.26(9)$, $b = 775.9(2)$, $c = 904.9(2)$ pm, $wR2 = 0.0425$, 485 F^2 values for $SrAu_3In_3$ and $a = 454.2(2)$, $b = 768.1(6)$, $c = 907.3(6)$ pm, $wR2 = 0.0495$, 551 F^2 values for $EuAu_3In_3$ with 26 variables for each refinement. The gold and indium atoms build up three-dimensional $[Au_3In_3]$ polyanionic networks, which leave distorted hexagonal channels for the strontium and europium atoms. Within the networks one observes Au2 atoms without Au–Au contacts and gold zig-zag chains (279 pm Au1–Au1 in $EuAu_3In_3$). The Au–In and In–In distances in $EuAu_3In_3$ range from 270 to 290 and from 305 to 355 pm. The europium atoms within the distorted hexagonal channels have coordination number 14 (8 Au + 6 In). $EuAu_3In_3$ shows Curie–Weiss behavior above 50 K with an experimental magnetic moment of 8.1(1) μB/Eu atom. ^{151}Eu Mössbauer spectra show a single signal at $\delta = -11.31(1)$ mm/s, compatible with divalent europium. No magnetic ordering was detected down to 3 K.

Keywords: Europium; Indium; Intermetallics; Mössbauer Spectroscopy

1. Introduction

Among the many rare earth (RE)–transition metal (*T*)–indides [1], those with europium play a special role. So far, the magnetic and ^{151}Eu Mössbauer spectroscopic data of $EuNiIn_4$ [2], $EuCuIn_4$ [3], EuZnIn [4], EuRhIn [5], $EuRhIn_2$ and $EuRh_2In_8$ [6], $EuPdIn_2$ [7], EuPdIn [8–10], EuPtIn [4,8], EuAuIn [8], and $Eu_2Au_3In_4$ [11] have been investigated. All of these europium compounds show stable divalent europium in $4f^7$ configuration and magnetic ordering at low temperatures. Even with the more electronegative gold atoms, these indides show no tendency for intermediate valence. We have now started a more systematic study of the Eu–Au–In system in the gold-rich part. Herein, we report on the new indide $EuAu_3In_3$ and isotypic $SrAu_3In_3$. $EuAu_3In_3$ is a further example for an indide with stable divalent europium.

2. Experimental

2.1. Synthesis

Starting materials for the preparation of $EuAu_3In_3$ and $SrAu_3In_3$ were sublimed ingots of europium (Johnson Matthey), a strontium rod (Johnson Matthey), gold wire (Degussa–Hüls), and indium tear drops, all with stated purities better than 99.9%. Pieces of the strontium rod were cut under paraffin oil, washed with n-hexane and kept in Schlenk tubes under argon prior to the reactions. The paraffin oil and *n*-hexane were dried over sodium wire. The argon was purified over titanium sponge (900 K), silica gel and molecular sieves. The elements were weighed in the ideal 1:3:3 atomic ratio and arc-welded [12] in small

*Corresponding author.
E-mail address: pottgen@uni-muenster.de (R. Pöttgen).

0022-4596/$ - see front matter © 2007 Elsevier Inc. All rights reserved.
doi:10.1016/j.jssc.2007.05.026

tantalum ampoules. The latter were placed in a water-cooled sample chamber [13] of an induction furnace (Hüttinger Elektronik, Freiburg, type TIG 1.5/300) under flowing argon and first annealed at 1400 K for 5 min followed by cooling to 900 K within 4 h. Finally, the temperature was kept at 900 K for another 4 h followed by quenching.

The samples were mechanically broken off the tantalum tubes. No reaction with the crucible material was evident. The compact and polycrystalline $EuAu_3In_3$ and $SrAu_3In_3$ samples are stable in air over weeks. Single crystals exhibit metallic lustre while ground powders are light gray. $EuAu_3In_3$ and $SrAu_3In_3$ were obtained in X-ray pure form in amounts of ca. 1 g.

2.2. X-ray powder data

Both samples were studied via Guinier powder patterns using Cu $K\alpha_1$ radiation and α-quartz ($a = 491.30$, $c = 540.46$ pm) as an internal standard. The Guinier camera was equipped with an imaging plate system (Fujifilm, BAS-1800). The orthorhombic lattice parameters (Table 1) were refined by least-squares calculations. The correct indexing of the experimental patterns was ensured by intensity calculations [14], taking the atomic sites derived from the single crystal data. The lattice parameters determined on the single-crystal diffractometer ($a = 453.8(1)$, $b = 768.2(1)$, $c = 907.9(1)$ pm for $EuAu_3In_3$ and $a = 454.35(9)$, $b = 773.5(2)$, $c = 908.7(2)$ pm for $SrAu_3In_3$) were close to the powder data.

Table 1
Crystal data and structure refinement for $SrAu_3In_3$ and $EuAu_3In_3$, space group *Pmmn*, $Z = 2$, Pearson symbol *oP*14

Empirical formula	$SrAu_3In_3$	$EuAu_3In_3$
Molar mass	1022.98	1087.32
Unit cell dimensions	$a = 455.26(9)$ pm	$a = 454.2(2)$ pm
(Guinier powder data)	$b = 775.9(2)$ pm	$b = 768.1(6)$ pm
	$c = 904.9(2)$ pm	$c = 907.3(6)$ pm
	$V = 0.3196\,nm^3$	$V = 0.3165\,nm^3$
Calculated density	$10.63\,g/cm^3$	$11.41\,g/cm^3$
Crystal size	$40 \times 70 \times 70\,\mu m^3$	$20 \times 40 \times 40\,\mu m^3$
Detector distance	100 mm	–
ω Range; incement	0–180°; 1.0°	–
Exposure time	5 min	–
Integr. Param. A, B, EMS	13.5; 3.5; 0.012	–
Transmission (max/min)	2.03	2.10
Absorption coefficient	$87.3\,mm^{-1}$	$89.6\,mm^{-1}$
F(000)	844	894
θ range for data collection	3–29°	2–30°
Range in *h k l*	$-6 \leqslant h \leqslant 6$	$-6 \leqslant h \leqslant 6$
	$-10 \leqslant k \leqslant 9$	$-10 \leqslant k \leqslant 10$
	$-12 \leqslant l \leqslant 10$	$-12 \leqslant l \leqslant 12$
Total no. of reflections	2911	3592
Independent reflections	485 ($R_{int} = 0.0526$)	551 ($R_{int} = 0.0797$)
Reflections with $I > 2\sigma(I)$	385	464
	($R_{sigma} = 0.0518$)	($R_{sigma} = 0.0377$)
Data/parameters	485/26	551/26
Goodness-of-fit on F^2	0.910	1.049
Final *R* indices [$I > 2\sigma(I)$]	$R1 = 0.0213$	$R1 = 0.0268$
	$wR2 = 0.0416$	$wR2 = 0.0469$
R indices (all data)	$R1 = 0.0312$	$R1 = 0.0389$
	$wR2 = 0.0425$	$wR2 = 0.0495$
Extinction coefficient	0.0129(5)	0.0065(2)
Largest diff. peak and hole	2.10 and $-2.47\,e/Å^3$	2.15 and $-4.09\,e/Å^3$

2.3. Single-crystal X-ray diffraction

Small single crystals of $EuAu_3In_3$ and $SrAu_3In_3$ were selected from the crushed samples after the annealing process. The crystals were glued to small quartz fibres using bees wax and then first checked by Laue photographs on a Buerger camera, equipped with the same Fujifilm, BAS-1800 imaging plate technique. Good-quality crystals of both indides were then used for the intensity data collections. The $SrAu_3In_3$ crystal was measured on a Stoe IPDS II diffractometer (graphite monochromatized Mo Kα radiation; oscillation mode). A numerical absorption correction was applied to the data set. Intensity data of $EuAu_3In_3$ were collected at room temperature by use of a four-circle diffractometer (CAD4) with graphite monochromatized Mo Kα radiation and a scintillation counter with pulse height discrimination. Scans were taken in the $\omega/2\theta$ mode. An empirical absorption correction was applied on the basis of Ψ-scan data, accompanied by a spherical absorption correction. All relevant crystallographic data for the data collections and evaluations are listed in Table 1.

2.4. Scanning electron microscopy

The single crystals investigated on the diffractometers and the bulk samples were analyzed using a LEICA 420 I scanning electron microscope with SrF_2, EuF_3, Au and InAs as standards. No impurity elements heavier than sodium were observed. The compositions determined by EDX (13 ± 2 at% Sr: 45 ± 2 at% Au: 42 ± 2 at% In and 13 ± 2 at% Eu: 44 ± 2 at% Au: 43 ± 2 at% In) are in good agreement with the ideal composition, i.e., 14.2:42.9:42.9. The standard uncertainties account for the analyses at various points.

2.5. Magnetic and spectroscopic data

The $EuAu_3In_3$ sample was packed in kapton foil and attached to the sample holder rod of a VSM for measuring the magnetic properties in a quantum design physical-property-measurement system in the temperature range 5–300 K with magnetic flux densities up to 80 kOe. For heat capacity (C_p) measurements (3–100 K) the sample was glued to the platform of a pre-calibrated heat capacity puck using *Apizeon N grease*.

The 21.53 keV transition of ^{151}Eu with an activity of 130 MBq (2% of the total activity of a $^{151}Sm:EuF_3$ source) was used for the Mössbauer spectroscopic experiments, which were conducted in the usual transmission geometry. The measurements were performed with a commercial helium bath cryostat at 4.2 and 77 K. The source was kept at room temperature. The sample was placed within a thin-

Table 2
Atomic coordinates and isotropic displacement parameters (pm^2) for $SrAu_3In_3$ and $EuAu_3In_3$

Atom	Wyckoff Site	x	y	z	U_{eq}
$SrAu_3In_3$					
Sr	2*b*	1/4	3/4	0.2694(2)	117(4)
Au1	4*e*	1/4	0.52383(7)	0.58763(6)	131(2)
Au2	2*a*	1/4	1/4	0.04449(9)	115(2)
In1	4*e*	1/4	0.55436(11)	0.88559(11)	84(2)
In2	2*a*	1/4	1/4	0.36673(15)	112(3)
$EuAu_3In_3$					
Eu	2*b*	1/4	3/4	0.26995(13)	128(2)
Au1	4*e*	1/4	0.52132(7)	0.58783(7)	146(2)
Au2	2*a*	1/4	1/4	0.04769(9)	122(2)
In1	4*e*	1/4	0.55172(11)	0.88380(12)	103(2)
In2	2*a*	1/4	1/4	0.36636(17)	121(3)

U_{eq} is defined as one third of the trace of the orthogonalized U_{ij} tensor.

walled PVC container at a thickness corresponding to about 10 mg Eu/cm^2.

3. Results and discussion

3.1. Structure determination and refinement

The structure of $SrAu_3In_3$ was determined first. Careful analyses of the IDPS data revealed a primitive orthorhombic unit cell and the observed systematic extinctions were compatible with space groups *Pmmn*, $Pm2_1n$ and $P2_1mn$, of which the centrosymmetric group was found to be correct during structure refinement. The starting atomic parameters were determined by an automatic interpretation of direct methods with SHELXS-97 [15] and the structure was refined with anisotropic displacement parameters for all atoms with SHELXL-97 (full-matrix least squares on F_o^2) [16]. The data of $SrAu_3In_3$ were then taken as starting parameters for refinement of the $EuAu_3In_3$ structure. The occupancy parameters have been refined in a separate series of least-squares cycles. All sites were fully occupied within two standard uncertainties and in the final cycles, the ideal occupancy parameters were assumed again. Final difference Fourier syntheses revealed no significant residual peaks. The refinement then converged to the residuals listed in Table 1 and the atomic parameters and interatomic distances listed in Tables 2 and 3. Further data on the structure refinements are available.[1]

3.2. Crystal chemistry

The indides $SrAu_3In_3$ and $EuAu_3In_3$ crystallize with a new orthorhombic structure type. So far, the indides $Sr_2Au_3In_4$, $Eu_2Au_3In_4$ [11], EuAuIn [5,8] and $EuAuIn_2$ [17] have been reported. As an example, the coordination polyhedra of the strontium compound are presented in Fig. 1. This structure type contains one strontium (europium), two gold and two indium sites. Together, the gold and indium atoms build up a three-dimensional $[Au_3In_3]$ network in which the strontium and europium atoms fill distorted hexagonal channels (Fig. 2). Within the network, one observes Au2 atoms without Au–Au interactions and gold zig-zag chains (279 pm Au1–Au1 in $EuAu_3In_3$). The latter Au–Au distances are even shorter than in *fcc* gold (288 pm Au–Au) [18].

Such gold zig-zag chains (282 pm Au–Au) also occur in the orthorhombic CrB-type structure of CaAu [19], where the gold atoms have trigonal prismatic calcium coordination. The structures of SrAu and BaAu [20] are stacking variants of FeB- and CrB-related slabs with stronger distortions. The various Au–Au distances in the crystallographically independent gold chains of SrAu range from 284 to 301 pm. Comparable Au1–Au distances of 283 pm occur in the Kagomé network of Rb_2Au_3 [21].

In various organogold compounds [22,23] dimeric units and chain structures are realized, and also a variety of homonuclear gold clusters [24] exists. The cluster compounds show a large range of Au–Au distances from 258 to 317 pm.

Table 3
Interatomic distances (pm) in the structures of $SrAu_3In_3$ and $EuAu_3In_3$, calculated with the lattice parameters obtained from X-ray powder data. Standard deviations are all equal or smaller than 0.3 pm

$SrAu_3In_3$				$EuAu_3In_3$			
Sr:	4	Au1	337.2	Eu:	4	Au1	334.2
	2	Au1	337.2		2	Au1	337.7
	4	In1	356.7		4	In1	353.2
	2	Au2	364.0		2	Au2	366.9
	2	In1	379.1		2	In1	382.0
Au1:	1	In1	270.7	Au1:	1	In1	269.6
	2	Au1	279.9		2	Au1	279.4
	2	In2	290.4		1	In2	289.5
	1	In2	291.7		2	In2	290.1
	2	Sr	337.2		2	Eu	334.2
	1	Sr	337.2		1	Eu	337.7
Au2:	2	In1	276.5	Au2:	2	In1	275.4
	4	In1	280.8		4	In1	280.4
	1	In2	291.6		1	In2	289.1
	2	Sr	364.0		2	Eu	366.9
In1:	1	Au1	270.7	In1:	1	Au1	269.6
	1	Au2	276.5		1	Au2	275.4
	2	Au2	280.8		2	Au2	280.4
	1	In1	303.6		1	In1	304.6
	2	In1	319.1		2	In1	319.9
	2	In2	356.4		2	Eu	353.2
	2	Sr	356.7		2	In2	355.4
	1	Sr	379.1		1	Eu	382.0
In2:	4	Au1	290.4	In2:	1	Au2	289.1
	1	Au2	291.6		2	Au1	289.5
	2	Au1	291.7		4	Au1	290.1
	4	In1	356.4		4	In1	355.4

All distances within the first coordination spheres are listed.

[1]Details may be obtained from: Fachinformationszentrum Karlsruhe, D-76344 Eggenstein–Leopoldshafen (Germany), by quoting the Registry nos. CSD–417876 ($SrAu_3In_3$) and CSD–417877 ($EuAu_3In_3$).

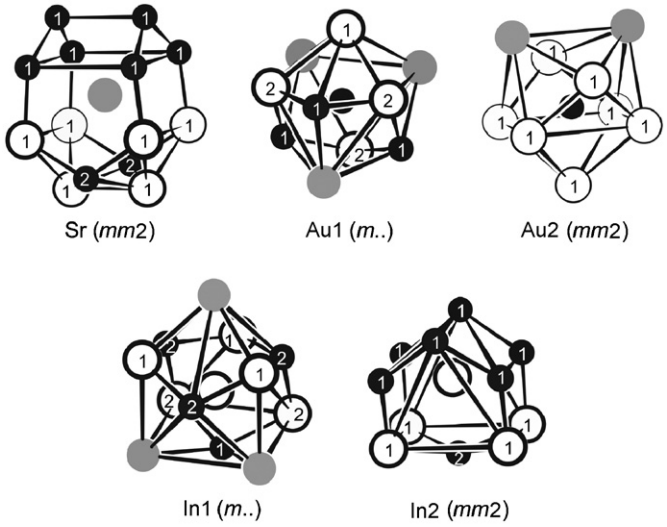

Fig. 1. Coordination polyhedra in the structure of $SrAu_3In_3$. Strontium, gold and indium atoms are drawn as medium gray, black filled and open circles, respectively. The site symmetries are indicated.

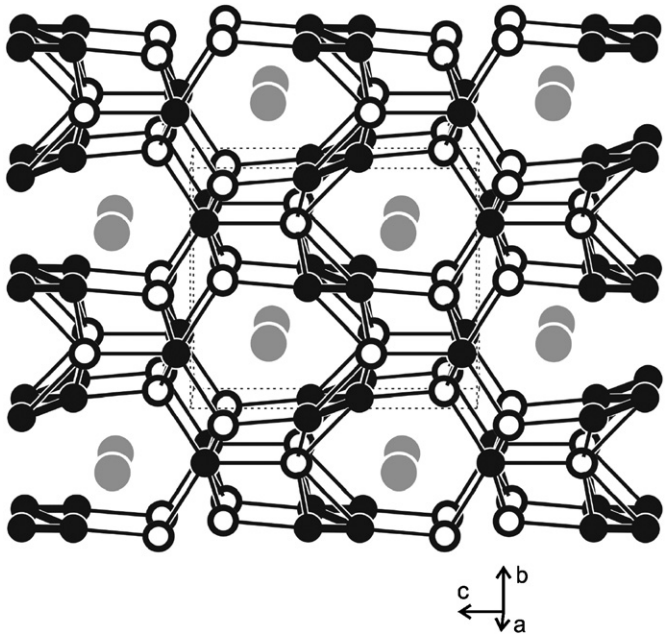

Fig. 2. View of the $SrAu_3In_3$ structure approximately along the *x*-axis. Strontium, gold and indium atoms are drawn as medium gray, black filled and open circles, respectively. The three-dimensional $[Au_3In_3]$ network is emphasized.

The Au1–Au1 zig-zag chains in $EuAu_3In_3$ are coordinated by indium atoms at shorter Au1–In distances ranging from 270 to 290 pm, close to the sum of the covalent radii of 284 pm [25]. Furthermore, the coordination sphere of the Au1 atoms is completed by three europium neighbors at 334 and 338 pm.

In contrast, the Au2 atoms have no Au–Au interactions. They have seven nearest-indium neighbors at Au2–In distances ranging from 275 to 289 pm, comparable to the Au1–In distances. Similar Au–In distances also occur in the structures of $Eu_2Au_3In_4$ [11], EuAuIn [5,8] and $EuAuIn_2$ [17]. We can thus assume substantial Au–In bonding within the three-dimensional $[Au_3In_3]$ network. Due to the high indium content, we also observe a variety of In–In distances (305–355 pm). These compare well with the structure of tetragonal body-centered indium (4×325 and 8×338 pm In–In) [18]. Consequently, Au–Au, Au–In as well as In–In bonding play a significant role in the three-dimensional $[Au_3In_3]$ network.

The three-dimensional $[Au_3In_3]$ networks leave distorted hexagonal channels that are filled by the strontium and europium atoms. The latter are bonded to the network via eight Sr–Au and Eu–Au contacts. For the strontium compound, the shorter Sr–Au distance of 337 pm is only slightly longer than the sum of the covalent radii of 326 pm [25]. They are comparable to the range of Sr–Au distances (318–346 pm) in SrAu [20]. The Sr–In and Eu–In distances are much longer (Table 3). Both the ranges of the Au–In distances and the coordination of the cations in $SrAu_3In_3$ and $EuAu_3In_3$ are similar to the many alkali metal–gold–indides [26–29] and references therein.

Finally, it is interesting to compare the $EuAu_3In_3$ structure with the orthorhombic $MgCuAl_2$-type structure of $EuAuIn_2$ [17]. In Fig. 3, we present projections of both structures along the short unit cell axis. The columns of the $EuAuIn_2$ structure also occur in the $EuAu_3In_3$ structure, however, they are separated by a slab of composition Au_2In, including the Au1–Au1 zig-zag chains. For both structures we observe similar ranges of Au–In and In–In distances, however, the europium atoms have closer Eu–Au (317–332 vs. 334–338 pm) and Eu–In (333–363 vs. 353–382 pm) contacts in $EuAuIn_2$. This might be a consequence of the higher europium content in $EuAuIn_2$.

From a purely geometrical point of view, the structure of $SrAu_3In_3$ can be described as a stacking of tetragonal (filled with strontium and indium atoms) and trigonal prisms (filled with gold and empty (*E*) ones) along the *z*-axis (Fig. 4). Summing up these slabs, the formula of $SrAu_3In_3$ is the following: $4EAu_{0.5} + 2AuIn_{0.5} + 2EIn_{0.5} + 2SrAu_{0.5}In_{0.5} + 2InAu_{0.5}In_{0.5} \equiv Sr_2Au_6In_6 = 2SrAu_3In_3$. Similar stacking sequences of this kind of slabs occur in the structures of $YbRhIn_4$ ($LaCoAl_4$ type), $EuPdIn_4$ ($YNiAl_4$ type), $EuAuIn_2$ ($MgCuAl_2$ type) and $Ce_2Au_3In_5$ (own type). An overview is given in [1].

The europium atoms as the most electropositive component in $EuAu_3In_3$ have transferred their two valence electrons (see magnetic and ^{151}Eu Mössbauer spectroscopic data below) to the gold and indium atoms, enabling the covalent bonding and formation of the three-dimensional $[Au_3In_3]$ polyanionic network. To a first approximation a formulation $Eu^{2+}[Au_3In_3]^{2-}$ is adequate.

3.3. Magnetic and ^{151}Eu Mössbauer spectroscopic data of $EuAu_3In_3$

The temperature dependence of the reciprocal magnetic susceptibility of $EuAu_3In_3$ is shown in Fig. 5. $EuAu_3In_3$ shows Curie–Weiss behavior above 50 K with an experimental

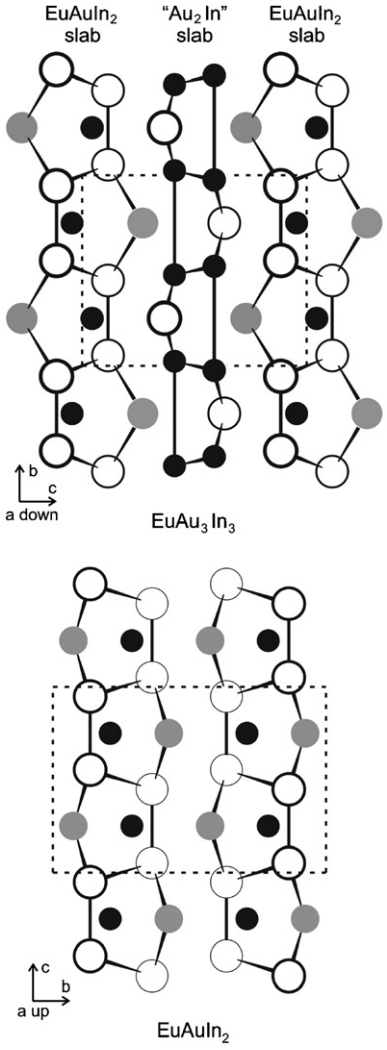

Fig. 3. Projections of the $EuAu_3In_3$ and $EuAuIn_2$ structures along the short unit cell axis. Europium, gold and indium atoms are drawn as medium gray, black filled and open circles, respectively. The common structural slabs are emphasized.

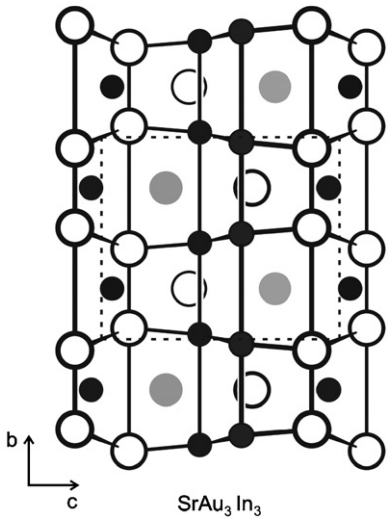

Fig. 4. View of the $SrAu_3In_3$ structure along the x-axis. Strontium, gold and indium atoms are drawn as medium gray, black filled and open circles, respectively. The distorted square and trigonal prismatic slabs are emphasized. They are stacked along the z-axis. For details see text.

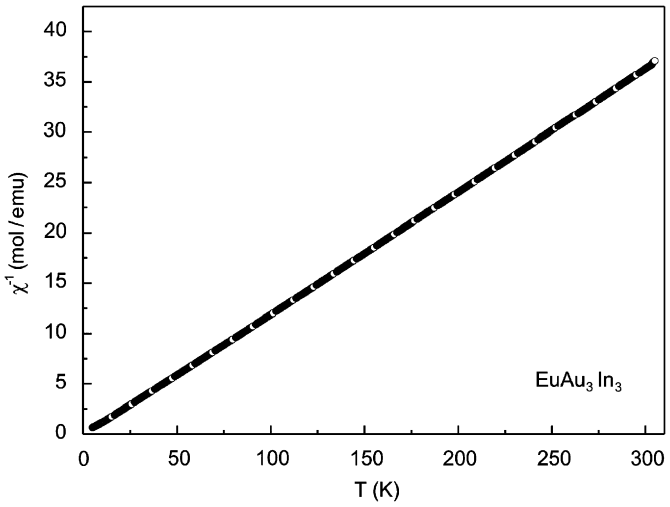

Fig. 5. Temperature dependence of the inverse magnetic susceptibility of $EuAu_3In_3$ measured at a magnetic flux density of 1 T.

magnetic moment of 8.1(1) μ_B/Eu atom and a small paramagnetic Curie temperature (Weiss constant) of 2.7(1) K, indicative for ferromagnetic interactions. The experimental magnetic moment is close to the free-ion value of 7.94 μ_B for Eu^{2+} [30].

The susceptibility data revealed no anomaly around 70 K where EuO orders ferromagnetically [31–33], indicating high purity of the sample. There was no hint for magnetic ordering in $EuAu_3In_3$ down to 5 K. In contrast, magnetic ordering at 21.0 and 9.5 K was observed for EuAuIn [8] and $Eu_2Au_3In_4$ [11]. The magnetization behavior of $EuAu_3In_3$ is shown in Fig. 6. At 50 K the magnetization curve is linear up the highest field of 8 T (2.1 μ_B/Eu atom), as expected for a paramagnetic material. The behavior is different at 5 K. Here, the magnetization increases linearly at low field and then shows a typical curvature with almost saturation at 8 T with a magnetic moment of 6.9 μ_B/Eu atom, close to the theoretical saturation magnetization of 7.0 μ_B/Eu atom according to $g \times S$ [30]. The external field forces the magnetic moments to parallel alignment. The 25 K curve is not linear, indicating that the magnetic interactions persist up to that temperature.

As a further hint for the magnetic behavior in $EuAu_3In_3$, we have measured the temperature dependence of the specific heat in the temperature range 3–100 K (Fig. 7). At low temperatures we observe a strong increase in C_P, indicating a lambda-type transition into a magnetically ordered state. The magnetic-ordering temperature is slightly below 3 K (temperature limit of the PPMS setup).

The ^{151}Eu Mössbauer spectra of $EuAu_3In_3$ at 4.2 and 77 K are shown in Fig. 8. Both spectra were well reproduced by single europium sites with almost similar fitting parameters: $\delta = -11.31(1)$ mm/s and $\Gamma = 2.73(4)$ mm/s at 77 K and $\delta = -11.26(2)$ mm/s and $\Gamma = 2.85(7)$ mm/s at

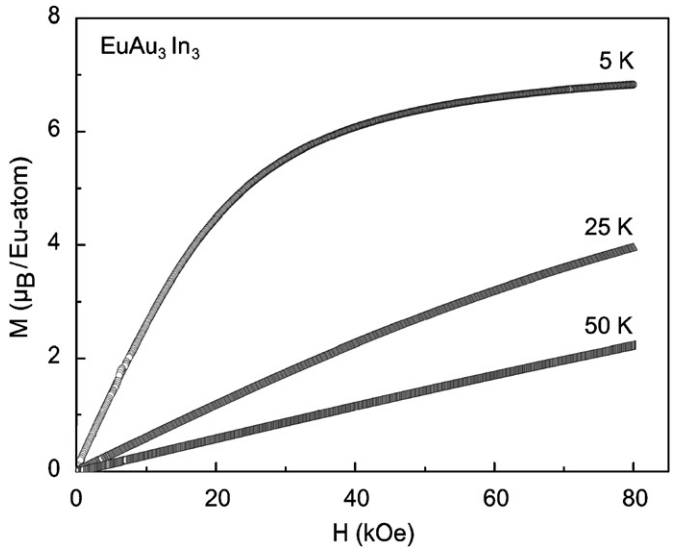

Fig. 6. Magnetization vs. field for $EuAu_3In_3$ at 5, 25, and 50 K.

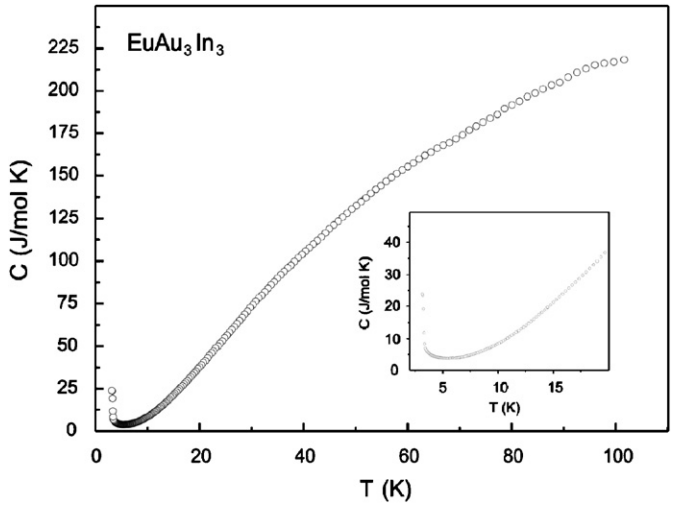

Fig. 7. Temperature dependence of the specific heat of $EuAu_3In_3$.

4.2 K, clearly indicating divalent europium (there is no contribution from a Eu^{III} species around 0 mm/s). The experimental line width at both temperatures is the same within one combined standard deviation. Thus, the 4.2 K Mössbauer spectrum gives no hint for a hyperfine field at the europium nuclei. Finally, it is interesting to compare the isomer shifts of EuAuIn (−9.9 mm/s) [4], $Eu_2Au_3In_4$ (−10.5 mm/s) [11] and $EuAu_3In_3$ (−11.3 mm/s). We observe a decrease of the effective *s* electron density from EuAuIn to $EuAu_3In_3$ indicating higher ionicity of the europium atoms in $EuAu_3In_3$, similar to the series of Eu*TX* compounds [34].

Acknowledgments

We are grateful to Dipl.-Ing. U. Ch. Rodewald and B. Heying for the intensity data collections. This work was supported by the Deutsche Forschungsgemeinschaft. I.R.M. is indebted to DAAD for a research stipend.

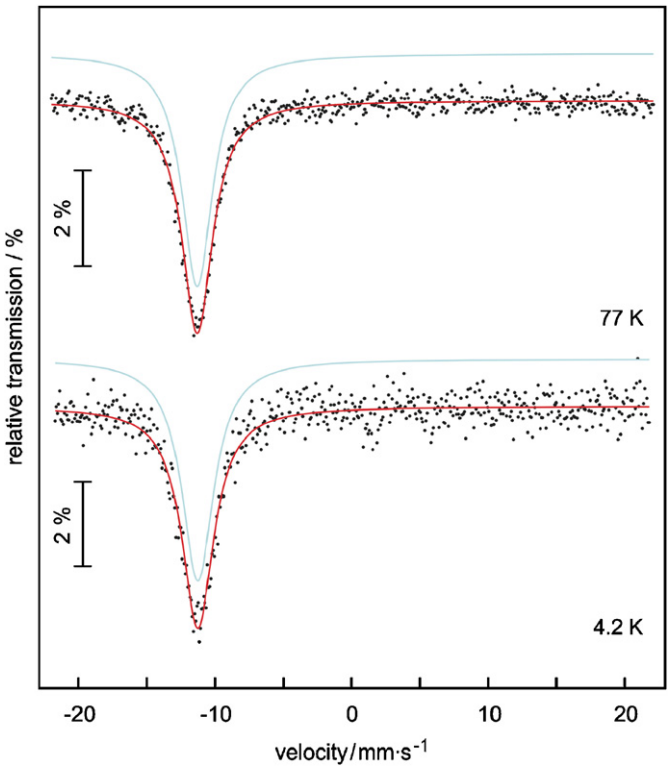

Fig. 8. Experimental and simulated ^{151}Eu Mössbauer spectra of $EuAu_3In_3$ at 77 and 4.2 K.

References

[1] Y.M. Kalychak, V.I. Zaremba, R. Pöttgen, M. Lukachuk, R.-D. Hoffmann, Rare earth-transition metal-indides, in: K.A. Gschneider Jr., V.K. Pecharsky, J.-C. Bünzli (Eds.), Handbook on the Physics and Chemistry of Rare Earths, vol. 34, Elsevier, Amsterdam, 2005, pp. 1–133 (Chapter 218).
[2] R. Pöttgen, R. Müllmann, B.D. Mosel, H. Eckert, J. Mater. Chem. 6 (1996) 801.
[3] R. Pöttgen, R.K. Kremer, W. Schnelle, R. Müllmann, B.D. Mosel, unpublished results.
[4] R. Müllmann, B.D. Mosel, H. Eckert, G. Kotzyba, R. Pöttgen, J. Solid State Chem. 137 (1998) 174.
[5] R. Pöttgen, R.-D. Hoffmann, M.H. Möller, G. Kotzyba, B. Künnen, C. Rosenhahn, B.D. Mosel, J. Solid State Chem. 145 (1999) 174.
[6] R. Pöttgen, D. Kußmann, Z. Anorg. Allg. Chem. 627 (2001) 55.
[7] Y.V. Galadzhun, R.-D. Hoffmann, G. Kotzyba, B. Künnen, R. Pöttgen, Eur. J. Inorg. Chem. (1999) 975.
[8] R. Pöttgen, J. Mater. Chem. 6 (1996) 63.
[9] S. Cirafici, A. Palenzona, F. Canepa, J. Less-Common Met. 107 (1985) 179.
[10] T. Ito, S. Nishigori, I. Hiromitsu, M. Kurisu, J. Magn. Magn. Mater. 177–181 (1998) 1079.
[11] R.-D. Hoffmann, R. Pöttgen, C. Rosenhahn, B.D. Mosel, B. Künnen, G. Kotzyba, J. Solid State Chem. 145 (1999) 283.
[12] R. Pöttgen, Th. Gulden, A. Simon, GIT Labor-Fachzeitschrift 43 (1999) 133.
[13] D. Kußmann, R.-D. Hoffmann, R. Pöttgen, Z. Anorg. Allg. Chem. 624 (1998) 1727.
[14] K. Yvon, W. Jeitschko, E. Parthé, J. Appl. Crystallogr. 10 (1977) 73.

[15] G.M. Sheldrick, SHELXS-97, Program for the Solution of Crystal Structures, University of Göttingen, Germany, 1997.
[16] G.M. Sheldrick, SHELXL-97, Program for Crystal Structure Refinement, University of Göttingen, Germany, 1997.
[17] R.-D. Hoffmann, R. Pöttgen, V.I. Zaremba, Ya.M. Kalychak, Z. Naturforsch. 55b (2000) 834.
[18] J. Donohue, The Structures of the Elements, Wiley, New York, 1974.
[19] F. Merlo, J. Less-Common Met. 86 (1982) 241.
[20] M.L. Fornasini, J. Solid State Chem. 59 (1985) 60.
[21] U. Zachwieja, J. Alloys Compds. 206 (1994) 277.
[22] A. Laguna, Gold compounds of phosphorous and the heavy group V elements, in: H. Schmidbaur (Ed.), Gold—Progress in Chemistry, Biochemistry and Technology, Wiley, Chichester, 1999 (Chapter 12).
[23] H. Schmidbaur, A. Grohmann, M.E. Olmos, Organogold chemistry, in: H. Schmidbaur (Ed.), Gold—Progress in Chemistry, Biochemistry and Technology, Wiley, Chichester, 1999 (Chapter 18).
[24] P.J. Dyson, D.M.P. Mingos, Homonuclear clusters and colloids of gold: synthesis, reactivity, structural and theoretical considerations, in: H. Schmidbaur (Ed.), Gold—Progress in Chemistry, Biochemistry and Technology, Wiley, Chichester, 1999 (Chapter 15).
[25] J. Emsley, The Elements, Oxford University Press, Oxford, 1999.
[26] U. Zachwieja, J. Alloys Compds. 235 (1996) 7.
[27] U. Zachwieja, J. Anorg. Allg. Chem. 622 (1996) 1581.
[28] B. Li, J.D. Corbett, Inorg. Chem. 45 (2006) 8958.
[29] B. Li, J.D. Corbett, J. Am. Chem. Soc. 128 (2006) 12392.
[30] H. Lueken, Magnetochemie, Teubner, Stuttgart, 1999.
[31] B.T. Matthias, R.M. Bozorth, J.H. Van Vleck, Phys. Rev. Lett. 5 (1961) 160.
[32] D.B. McWhan, P.C. Souers, G. Jura, Phys. Rev. 143 (1966) 385.
[33] B. Stroka, J. Wosnitza, E. Scheer, H.v. Löhneysen, W. Park, K. Fischer, Z. Phys. B: Condens. Matter 89 (1992) 39.
[34] R. Müllmann, U. Ernet, B.D. Mosel, H. Eckert, R.K. Kremer, R.-D. Hoffmann, R. Pöttgen, J. Mater. Chem. 11 (2001) 1133.